Biosensors and Bioelectronics 53 (2014) 12–17

Contents lists available at ScienceDirect

Biosensors and Bioelectronics

journal homepage: www.elsevier.com/locate/bios

Label-free electrochemical biosensor using home-made 10-methyl-3-nitro-acridone as indicator for picomolar detection of nuclear factor kappa B

Jing Hua Chen [a,*], Xi Zhang [a], Shuxian Cai [a], Dongzhi Wu [a], Jia Lin [a], Chunyan Li [a], Jing Zhang [b,*]

[a] Department of Pharmaceutical Analysis, Faculty of Pharmacy, Fujian Medical University, Fuzhou, Fujian 350004, China
[b] Department of Chemistry and Biology, Faculty of Life Science, Fujian Agriculture and Forestry University, Fuzhou, Fujian 350002, China

ARTICLE INFO

Article history:
Received 20 July 2013
Received in revised form
5 September 2013
Accepted 17 September 2013
Available online 25 September 2013

Keywords:
Electrochemical biosensor
10-methyl-3-nitro-acridone
Nuclear factor kappa B

ABSTRACT

A new acridone derivative 10-methyl-3-nitro-acridone (MNA) with excellent electrochemical activity was synthesized in this paper. Using it as an electrochemical indicator, a signal-on and label-free electrochemical biosensor was developed for picomolar determination of nuclear factor kappa B (NF-κB) in serum. Initially, linear double-stranded DNA (dsDNA) probes, which contain a protein-binding site specific to NF-κB, were self-assembled on the surface of a glass carbon electrode (GCE). If the NF-κB was absent, the dsDNA probes were cut into ss-DNA fragments by the digestion of ExoIII, resulting in a low electrochemical signal of MNA due to the weak binding affinity of MNA to ss-DNA. On the contrary, in the presence of NF-κB, it could bind with the dsDNA probes at the specific site and hinder the digestion of ExoIII, resulting in a significant increase of electrochemical response due to the intercalation of MNA into the dsDNA probes. By employing the above strategy, this sensor could detect as low as 40 pM NF-κB with high specificity. To the best of our knowledge, the proposed sensor is the first attempt to use acridone derivative as an electrochemical indicator for NF-κB detection, which may represent a promising path toward clinical diagnosis and drug developments.

1. Introduction

Transcription factors are one of the largest classes of sequence-specific DNA-binding proteins, regulating cell development, differentiation, growth, and physiology (Papavassiliou, 1995). As a family of transcription factor, NF-κB, which influences a large number of genes expression and closely related to many diseases including asthma, cancer and diabetes, has already become the focus of intense research nowadays (Kumar et al., 2004; Hayden and Ghosh, 2008). Therefore, the sensitive, rapid and convenient detection of NF-κB levels is of great importance for drug developments and the early diagnosis or prevention of many diseases (Perkins, 2007; Hayden and Ghosh, 2004).

The conventional method for detecting NF-κB protein is electrophoretic mobility shift assay (EMSA) (Schmid et al., 1994). However, EMSA is tedious, time-consuming, radioactive and poorly reproducible. Recently, some new alternatives to the EMSA have been proposed such as immunoassay (Wang et al.,2006; Wang et al., 2008), fluorescence techniques (Ma et al., 2011; Liu et al., 2012), atomic force microscopy (AFM) (Menotta et al., 2010). Nevertheless, these methods usually need specific NF-κB antibodies, expensive fluorescence probes, laborious labeling techniques or special instruments, which hinder them from more extensive applications. So it is urgently needed to develop more sensitive, cost-effective, rapid, and miniaturized, easily operated methods for NF-κB quantification.

In an attempt to overcome the above disadvantages, several novel electrochemical biosensors for NF-κB detection have been developed due to simplicity and high sensitivity. For example, Pan et al. proposed an electrochemical approach for detection of NF-κB by combining Taq enzyme-mediated elongation and gold nanoparticle (AuNPs)-catalyzed silver enhancement (Pan et al., 2008). Although the method can detect NF-κB down to 0.1 pM with pronounced specificity, the prerequisite complicated and precise control of the experimental conditions make it lack of simplicity and practicability. Shen et al. developed a novel electrochemical sensor for NF-κB detection based on triplex DNA and gold nanoparticles (Shen et al., 2012). Although the sensor was simple, cheap and regenerated, the detection limit of the signal-off strategy has remained in need of further improvement for practical applications.

* Corresponding authors. Tel./fax: +86 591 228 62 016.
E-mail addresses: cjh_huaxue@126.com (J.H. Chen), 1601225385@qq.com (J. Zhang).

0956-5663/$ - see front matter © 2013 Elsevier B.V. All rights reserved.
http://dx.doi.org/10.1016/j.bios.2013.09.038

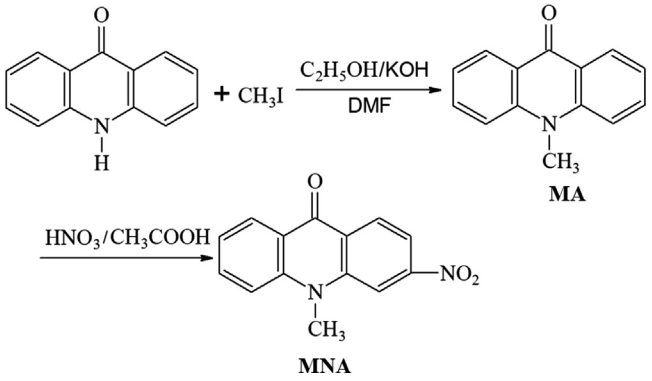

Fig. 1. Synthesis route of MNA.

Acridine and acridone derivatives possess strong and stable fluorescent emission and their planar structure confers on these molecules the ability to bind DNA by intercalation, which enable them to be used as fluorescent labels for peptides and amino acids (Faller et al., 1997; Reymond et al., 1996). Due to the known electrochemical activity of acridone, our group recently has focused on the synthesis of some new acridone derivatives in order to apply them into electrochemical fields. For example, we previously designed and synthesized an acridone derivative 2-nitroacridone (NAD), which possesses electrochemical activity with a couple reversible redox peaks on the GCE. Using NAD as the electrochemical indicator, two biosensors for DNA species detection were developed (Chen et al., 2008a, 2008b). Nevertheless, NAD exhibits high electrochemical activity only in acidic condition but poorly in neutral condition closed to the physiological environment, which makes it not suitable to be used as an excellent electrochemical indicator in biomedical field. Consequently, based on the previous work, we herein prepared a novel acridone derivative MNA (see Fig. 1) with excellent and stable electrochemical activity in neutral condition. Furthermore, because to its binding affinity to dsDNA chains is more efficient than to ss-DNA, MNA can be used as a hybridization indicator in the fabrication of the electrochemical biosensors. Compared with the commonly used electrochemical indicator containing metal ions, such as ruthenium, osmium, iridium and platinum complexes (Lim et al., 2009; Holmlin et al., 1996; Shao and Barton, 2007; Ma et al.; 2009), which need difficult, time-consuming and expensive procedures of the complexes synthesis, the small molecule of MNA can be easily prepared with high yield using inexpensive materials. All the above properties make MNA have more potential biomedical applications in the future. Therefore, based on the outstanding electrochemical stability and biocompatibility of MNA, we herein develop a signal-on electrochemical biosensor for label free detection of NF-κB in serum. To the best of our knowledge, this is the first study to use acridone derivatives for NF-κB detection. Combined with the advantages of electrochemical biosensors, such as fabrication easiness, operation convenience, portable, fast and low cost, our proposed sensor may represent a promising path toward direct NF-κB detection. In addition, we envision that the proposed biosensor holds great potential to be used in a wide variety of DNA-binding transcription factors only by changing the binding sequence and rational selecting exonuclease.

2. Experimental section

2.1. Apparatus

The Fourier transform infrared (FT-IR) experiment was carried out on a Perkin-Elmer Spectrum 2000 FT-IR spectrometer in a KBr pellet. Elemental analysis was performed on an elemental analyzer (Elementarvario EL□). Mass spectra (ESI) were measured by a Thermo Finnigan DECAX-30000 LCQ Deca XP ion trap mass spectrometry. UV/vis absorbance spectra were measured with a UV-2501PC spectrophotometer (SHIMADZU, Japan) using a quartz cell with 1.0 cm optical pathway. All electrochemical measurements were performed by using CHI 660D Electrochemical Workstation (CH Instrument, USA). The electrochemical system consisted of a working electrode (GCE), an auxiliary electrode (platinum wire), and a reference electrode (Ag/AgCl). The cyclic voltammetrys (CVs) scanning was performed in the potential range of $-0.4\sim+0.4$ V with a scanning rate of 100 mV/s. For square wave voltammetrys (SWVs) scanning, the potential scanning range was from -0.4 to $+0.06$ V; square wave frequency was 10 Hz; the square wave amplitude was 50 mV and scan potential increment was 2 s.

2.2. Reagents

Acridone (A.R), N,N-dimethyl formamide (DMF), 1-Ethyl-3-(3-dimethyllaminopropyl) carbodiimide hydrochloride(EDC), N-hydroxysulfosuccinimide sodium salt (NHS), methyl iodide, and bovine serum albumin (BSA) (99%) were purchased from Sigma without further purification. Nuclear factor kappa B (NF-κB) (p50) was obtained from Promega. Exonuclease III (ExoIII) and 1 × NE Buffer (10 mM Bis Tris Propane-HCl, 10 mM $MgCl_2$, 1 mM dithiothreitol, pH 7.0) was purchased from New England Biolabs. Oridonin was purchased from National Institute for the Control of Pharmaceutical and Biological Products, Beijing, China. The DNA-binding buffer was the mixture of 10 mM Tris–HCl (pH 7.5), 50 mM NaCl, 0.5 mM EDTA, 0.5 mM DTT, 3 mM $MgCl_2$, 0.05 mg/mL poly(dI-dC), 10% v/v glycerol, 0.5 mg/mL BSA, and 0.05% NP-40. Phosphate buffer solutions (PBS) with different pH were prepared by mixing the stock solutions of 0.05 mol L^{-1} NaCl and 0.1 mol L^{-1} NaH_2PO_4–Na_2HPO_4, and then adjusting the pH with 0.1 mol L^{-1} H_3PO_4 or 0.1 mol L^{-1} NaOH. All oligonucleotides were synthesized by Sangong Biotech (Shanghai, China) Co., Ltd., and their base sequences were illustrated in Table S1. All other reagents were of analytical reagent grade and MilliQ water (18.2 MΩ) was used throughout.

2.3. Preparation of MNA

As shown in Fig. 1, 10-methyl-acridone (MA) was synthesized starting with 9(10H)-acridone. An amount of 1.0 g 9(10H)-acridone was put into a beaker and dissolved in the hot potassium ethoxide solution. After distilling the ethanol, 12.5 mL DMF was added into the above solution with the temperature rising to 160 °C. Then 1.0 mL methyl iodide was added to react for 10 min under stirring. Subsequently, the as-prepared solution was poured into ice water to precipitate. After filtering off, washing with some water and further purifying by recrystallization in absolute alcohol, the resulted solid precipitate was oven-dried at 70 °C until yellow crystal MA was obtained.

MNA was synthesized starting with MA. 0.75 g of MA was put into a beaker with 50 mL of 36% acetic acid, 3.6 mL nitric acid and 8 mL glacial acetic acid added together. Then the temperature was raised to 55–60 °C and the reaction was performed for 2 h under stirring. Subsequently, the solution was poured into ice water and a solid precipitate appeared. After filtering off, washing with some water and further purifying by recrystallization in absolute alcohol, the resulted solid was oven-dried at 70 °C until yellow crystal MNA obtained. Analytical for MNA: C, 66.22%; H, 4.12%; N, 11.02%. (calculated: C, 66.14%; H, 3.94%; N, 11.02%); IR (KBr) ν: 2970, 2860 (υ_{CH3}), 1584 (υ_{C-C}), 1650 ($\upsilon_{C=C}$), 1380 ($\upsilon_{C\text{-}NO2}$). MS: m/z 255 ($[M+1]^+$). ^{1}H NMR ($CDCl_3$, δ) 7.82 (d, ArH), 7.64 (s, ArH), 7.62

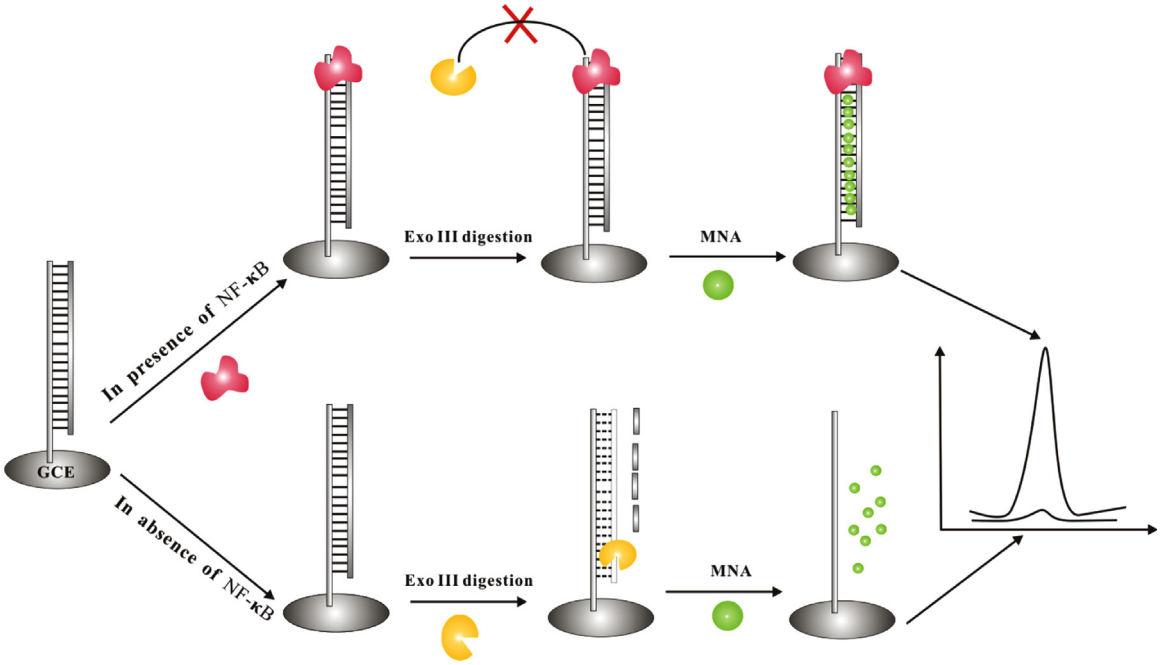

Fig. 2. Experimental principle of the electrochemical biosensor.

(t, ArH), 7.48 (d, ArH), 6.92 (d, ArH), 6.76 (t, ArH), 6.50 (d, ArH), and 2.72 (m, CH_3).

2.4. Electrochemical behavior of MNA

The GCE was mechanically polished with 0.05 μM Al_2O_3 slurry, and then washed ultrasonically in nitric acid followed by ethanol and water for a few minutes. Subsequently, 10 μL of 1.0 mM MNA was diluted to 10 mL with PBS (pH 7.0) buffer solution in a dry 10 mL electrochemical cell. After standing for 20 min, the CVs characteristics of the resulted mixture were investigated.

2.5. Preparation of the electrochemical biosensor

The scheme for preparation of the electrochemical biosensor is shown in Fig. 2. Prior to the experiment, the GCE was first polished using 1.0 μm, 0.3 μm and 0.05 μm Al_2O_3 suspensions and then extensively rinsed in water ultrasonically. Afterwards, the electrode was oxidized at +0.50 V for 1 min in 50 mM PBS (pH 7.40), followed by thorough rinsing with water. Then 20 μL of solution containing 5 mM EDC and 8 mM NHS in 50 mM PBS (pH 7.40) was pipetted onto the GCE surface. After air-drying and rinsing with water, the surface of GCE was drop-coated with S1. Following air-drying and rinsing with water to eliminate the adsorbed S1, S1-modified GCE was immersed in PBS buffer containing complementary S2 to hybridize for 2 h. After drying at room temperature and thoroughly rinsing with PBS buffer and water successively to eliminate the adsorbed S2, the dsDNA probe-modified GCE was immersed in DNA-binding buffer containing NF-κB at 37 °C for 30 min while stirring. Then 40 units of ExoIII were added for an additional 5 min at 37 °C. After EDTA was added to a final concentration of 20 mM to terminate the ExoIII reaction, the GCE was rinsed with the PBS buffer and water successively. Finally, the resulted GCE was immediately immersed in 1.0 μM MNA solution for 5 min at room temperature and rinsed successively. The electrochemical measurements were carried out in a 10 mL electrochemical cell.

3. Results and discussion

3.1. Experimental principle of the electrochemical biosensor

The proposed biosensor combined the outstanding electrochemical character of MNA and 3′→5′ activity of ExoIII for the detection of NF-κB. MNA has a double strand-specificity with higher binding affinity to dsDNA than to ss-DNA. ExoIII also has a double strand-specificity which selectively digests dsDNA from 3′-OH blunt or recessed end. As shown in Fig. 2, the linear dsDNA probe consists of two reverse complementary oligonucleotides (S1 and S2). One side of the probe contains one protein-binding site and the other side of it is labeled with the amino-group. Initially, the dsDNA probe is immobilized on the carboxy modified GCE surface through covalent combination. If the NF-κB is absent, ExoIII gradually digests the dsDNA probe from 3′-OH blunt end specifically, resulting in the formation of ss-DNA fragments. Due to the weak binding affinity of MNA to ss-DNA, the electrochemical signal of MNA is very small. However, in the presence of NF-κB, it can bind to the dsDNA probe at the protein-binding site, leading to a physical hindrance to ExoIII. As a result, the dsDNA probe retains its double-stranded structure. Then the MNA will intercalate into the double-stranded DNA substrate, resulting in a significant increase of electrochemical response. Using this sensing platform, an ultra-highly sensitive and selective, turn-on, label-free simple, rapid electrochemical biosensor for the detection of NF-κB has been developed.

3.2. Electrochemical behavior of MNA

Fig. S1 shows CVs of MNA in PBS (pH 7.0) with 100 mV s^{-1} of scan rate. As shown, there is a good peak shape in the range of −0.4 ~ +0.4 V. The cathodic peak potential (E_{pc}) and the anodic peak potential (E_{pa}) are −0.1382 V and −0.1099 V, respectively. The anodic peak current (I_{pa}) against the cathodic peak current (I_{pc}) is about 1, indicating the reaction is reversible. The number of electrons (n) involved in the reaction is about 2 according to $\Delta E_p = 2.3RT/nF$ (59/n mV at 25 °C) due to $\Delta E_p = 28.3$ mV (Bard and Faulkner, 1980). At the same time, an approximate estimation of n

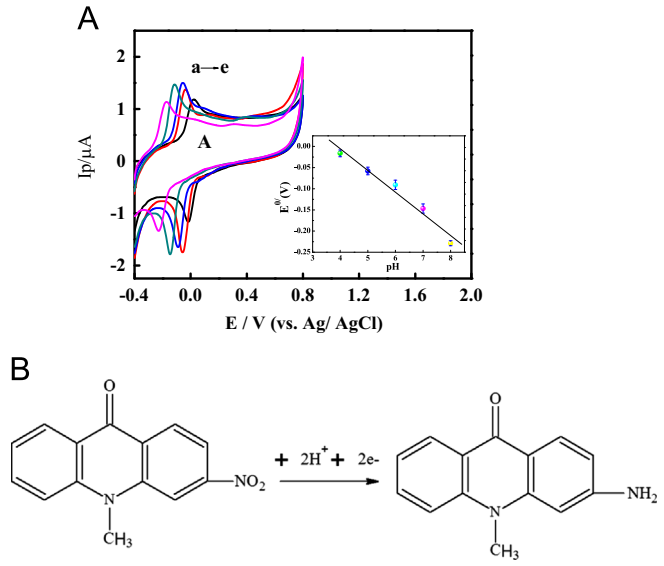

Fig. 3. (A) The CVs of MNA in the presence of different pH. a–e: 8; 7; 6; 5; and 4. Inset: the relationship between pH and the $E^{o'}$. (B) Electrochemical reaction mechanism of MNA.

is also calculated by the method used by Sharp et al. (1979). $I_p = n^2F^2A\Gamma\nu/4RT = nFQ\nu/4RT$; $Q = nFA\Gamma$; $S = Q\nu$, where A is the geometric surface area of the electrode, Γ (mol cm^{-2}) is the surface coverage, ν is the scan rate, and other symbols have their usual meanings. Through calculation, n is also two, which is in good agreement with the results obtained from the above method.

The effect of scan rate on the peak current of MNA was also studied. The experimental result showed that I_{pa} and I_{pc} increase with the increasing scan rate. Moreover, the peak current is proportional to the scan rate over the range of 20–300 mV/s, which suggests that the electrochemical reaction is an adsorption-controlled process in the solution (Chen et al., 2007a).

To further investigate the mechanism of electrochemical reactions of MNA on the electrode, the effect of pH on the formal potential ($E^{o'}$) was investigated using CVs. The CVs show $E^{o'}$ shifts to a more negative potential with the increasing pH (Fig. 3A), which indicate that the protons are involved in the reaction process on the GCE. The plot of the $E^{o'}$ versus pH shows linearity in the pH range of 4.0–8.0 and the linear regression equation is $E^{\circ\prime} = -0.0559\ \mathrm{pH} + 0.2948$ (the inset of Fig. 3A). Due to the formula of the slope = $0.059m/n$ (Chen et al., 2007b) (n is the number of electrons transfer, m is the number of protons transfer), the number of protons involved is also predicted to be two. So the electron transfer number is equal to the proton number participating in the reduction reaction. According to the references Marquez and Pletcher (1980), the electrochemical reactive mechanism of MNA is illustrated in Fig. 3B.

3.3. UV–vis absorption spectrum and electrochemical studies on the interaction between MNA and dsDNA or ssDNA

The interaction between MNA and dsDNA or ssDNA was studied by the UV–vis absorption spectrum. As shown in Fig. S2, the absorption peak of MNA (curve a) decreased slightly after the addition of ssDNA(curve b) while decreased significantly with a slight red shift after the addition of dsDNA (curve c), indicating possible intercalation of MNA into dsDNA strands (Long and Huang, 2007). The above results might vary because, upon binding with dsDNA, the planar anthraquinone ring of MNA could slide into adjacent base pairs (Zhou et al., 2005) and would be unable to H bond with the solvent water molecules. However, the random coil-like, disordered ssDNA without adjacent base pairs does not provide a favorable environment for MNA intercalation.

In addition, Carter et al. have previously demonstrated that intercalative binding of small molecules to DNA might make $E^{\circ\prime}$ shift to more positive value, while electrostatic binding might make $E^{\circ\prime}$ shift to more negative value. After MNA reacted with dsDNA for 15 min, both the cathodic and anodic $E^{o'}$ shifted toward the positive direction with their peak currents decreased meantime. However, the shift of $E^{o'}$ was neglectable upon the addition of ssDNA into MNA. Therefore, MNA intercalate into dsDNA, which corresponds with the above UV–vis results (Cusumano et al., 2006).

3.4. The specificity of the biosensor

To characterize the specificity of the biosensor, we replaced NF-κB with BSA without binding site as a control protein. As shown in Fig. 4, compared with the background signal (in the absence of NF-κB, curve e), NF-κB led to obvious current signal change by 3.1-fold (curve a) while the change of signal for BSA (10-fold higher than NF-κB concentration) was negligible (curve c). To further prove that the inhibition of ExoIII digestion was due to the selective binding of the dsDNA probe with NF-κB, we replaced the dsDNA probe with a dsDNA probe without NF-κB binding site (control dsDNA). The result showed that control dsDNA nearly did not affect the current signal (curve d). In addition, oridonin, a known inhibitor for the binding activity between NF-κB and DNA (Leung et al., 2005), was selected as a model inhibitor to demonstrate the selective binding of NF-κB with the dsDNA probe. As shown in curve b of Fig. 4, upon addition of 20 μM oridonin, a significant decrease of the current response of MNA in the presence of 0.5 nM NF-κB was observed, demonstrating that the biosenor did work as we expected. All the above observations led to the conclusion that the proposed biosensor exhibited an excellent specificity due to the highly specific interaction of the dsDNA probe and NF-κB, as well as the highly discriminative ability of ExoIII for the dsDNA with and without NF-kB. Moreover the label-free and simple biosensor also showed great potential to be readily applied to the large scale screening of small molecule inhibitors of NF-κB.

3.5. Optimization of experimental conditions

Experimental variables affecting the whole sensing process were optimized. First, the effect of MNA concentration on the net current (ΔI_p, the current of MNA minus that of the background) was investigated. ΔI_p increases with the increase of MNA concentration up to 1.0 μM while decreases for higher concentrations, so it was used for subsequent detection. Second, the concentration of ExoII

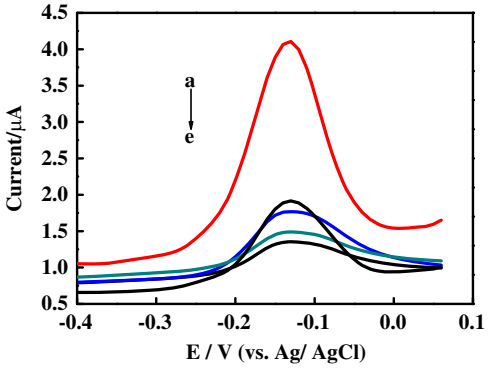

Fig. 4. The SWVs of the dsDNA probe modified GCE in the presence of 0.5 nM NF-κB (a), 20 μM oridonin (b), 5 nM BSA (c) or in the absence of NF-κB (e) and the control dsDNA modified GCE in the presence of 0.5 nM NF-κB (d).

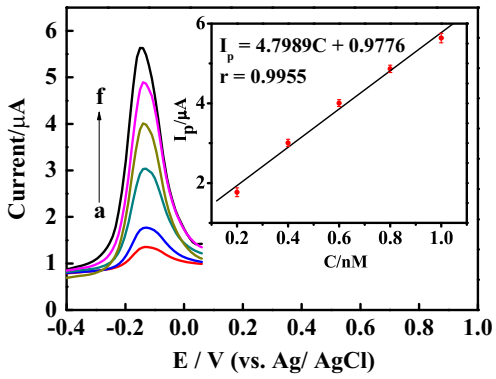

Fig. 5. SWVs of MNA for different concentrations of NF-κB in PBS (pH 7.0), a–f:0; 0.2; 0.4; 0.6; 0.8; 1.0 nM, Inset: relationship curves of concentration of NF-κB versus I_p. Error bars show the standard deviation of five experiments, and the values of 0.2, 0.4, 0.6, 0.8 and 1.0 nM were 6.2%, 3.1%, 2.1%, 1.9% and 2.1%, respectively.

Table 1
Determination of NF-κB in artificial serum sample (n=5).

Target NF-κB added (nM)	Detected by this method (nM)	Recovery of this method (%)	RSD (%)
0.4	0.37	92.5	6.1
0.6	0.58	96.7	5.7
0.8	0.84	105.2	4.1

and its reactive time were also tested. The results showed that ΔI_p reached a maximum when 20 U/mL ExoIII was added to the reaction system for 5 min. Finally, the effect of other experimental variables such as buffer type and pH of the buffer were also examined in detail. The results showed that the optimum conditions were PBS and 7.0, respectively.

3.6. The sensitivity of the biosensor

The sensitivity of the biosensor for accurate quantification of NF-κB was investigated by varying the concentration of NF-κB under the optimized assay conditions. Due to the fact that NF-κB could protect the dsDNA probe from being degraded by ExoIII, the MNA can intercalate into the dsDNA resulting in the increase in current intensity. As expected, the addition of an increasing amount of NF-κB resulted in a dynamic increase in current signal (Fig. 5). A linear relationship between I_p and the concentration of NF-κB (C) was plotted (inset of Fig. 5) in the range of 0.2–1.0 nM. The calibration equation obtained from this curve was I_p=4.7989C+ 0.9776 with a correlation coefficient of 0.9955 (inset in Fig. 5). The calculated limit of detection (LOD) was 40 pM with a signal-to-noise ratio of 3. Compared to the existing electrochemical methods (Pan et al., 2008; Shen et al., 2012), the proposed label-free biosensor is simpler, faster and cheaper. Moreover, in comparison with the former fluorescent methods (Liu et al., 2012), the biosensor possesses better sensitivity because it requires no fluorescent labeling, which not only decreases the background signal by preventing the labeling moieties from interfering with protein binding but also simplifies the fabrication of the sensors and lowers cost.

3.7. Detection of artificial serum sample

In order to evaluate the practical applicability and accuracy, the biosensor was used for determining the recoveries by dissolving three different concentrations of NF-κB into the fetal calf serum. The recoveries were calculated in Table 1 by the found amount/added amount ratio. The above results verified that the proposed biosensor can be applied to the quantitative determination of NF-κB in serum.

4. Conclusions

In this work, we developed an electrochemical biosensor with MNA as an electrochemical indicator for the determination of NF-κB for the first time. The introduction of MNA makes the sensor not require fluorophore- and quencher-modified nucleotides near the binding site, which not only simplifies fabrication of the sensors and lowers cost, but also prevents the interference from the labeling moieties. Moreover, compared with the signal-off methods, the signal-on sensor can obtain higher sensitivity with the detection limit of NF-κB down to 40 pM. In addition, the sensor can be used in monitoring other DNA-binding transcription factors only through rationally designing dsDNA probe according to the various targets. In summary, due to its high sensitivity and selectivity, easy-to-use, fast and inexpensive features, the proposed sensor may have a promising clinical potential application in the future.

Acknowledgments

The authors gratefully acknowledge the financial support of the National Natural Science Foundation of China (21105012, 21205015, 21375017), the National Science Foundation for Distinguished Young Scholars of Fujian Province (2013J06003), the Key Project of Fujian Science and Technology (2013Y0045), National Science Foundation of Fujian Province (2011J01028), Program for Fujian University Outstanding Youth Scientific Research (JA11105, JA10295), the Foundation of Fuzhou Science and Technology Bureau (2012-S-148).

Appendix A. Supplementary material

Supplementary data associated with this article can be found in the online version at http://dx.doi.org/10.1016/j.bios.2013.09.038.

References

Bard, A.J., Faulkner, L.R., 1980. Electrochemical Methods, Fundamentals and Applications. Wiley, New York p. 157.
Chen, J., Zhang, J., Huang, L., Lin, X., Chen, G., 2008a. Biosensors and Bioelectronics 24, 349–355.
Chen, J., Zhang, J., Wang, K., Huang, L., Lin, X., Chen, G., 2008b. Electrochemistry Communications 10, 1448–1451.
Chen, J.H., Zhang, J., Zhuang, Q., Chen, J., Lin, X.H., 2007b. Electroanalysis 17, 1765–1772.
Chen, J.H., Zhang, J., Zhuang, Q., Zhang, S.B., Lin, X.H., 2007a. Talanta 72, 1805–1810.
Cusumano, M., DiPietro, M.L., Giannetto, A., 2006. Inorganic Chemistry 45, 230–235.
Faller, T., Hutton, K., Okafo, G., Gribble, A., Camilleri, P., Games, D.F., 1997. Chemical Communications, 1529–1530.
Hayden, M.S., Ghosh, S., 2004. Genes and Development 18, 2195–2224.
Hayden, M.S., Ghosh, S., 2008. Cell 132, 344–362.
Holmlin, R.E., Stemp, E.D.A., Barton, J.K., 1996. Journal of the American Chemical Society 118, 5236–5244.
Kumar, A., Takada, Y., Boriek, A.M., Aggarwal, B.B., 2004. Journal of Molecular Medicine 82, 434–448.
Leung, C.H., Grill, S.P., Lam, W., Han, Q.B., Sun, H.D., Cheng, Y.C., 2005. Molecular Pharmacology 68, 286–297.
Lim, M.H., Song, H., Olmon, E.D., Dervan, E.E., Barton, J.K., 2009. Inorganic Chemistry 48, 5392–5397.
Liu, J.J., Song, X.R., Wang, Y.W., Chen, G.N., Yang, H.H., 2012. Nanoscale 4, 3655–3659.
Long, Y.F., Huang, C.Z., 2007. Talanta 71, 1939–1943.
Ma, D.L., Che, C.M., Yan, S.C., 2009. Journal of the American Chemical Society 131, 1835–1846.
Ma, D.L., Xu, T., Chan, D.S., Man, B.Y., Fong, W.F., Leung, C.H., 2011. Nucleic Acids Research 39, e67.

Marquez, J., Pletcher, D., 1980. Journal of Applied Electrochemistry 10, 567–573.
Menotta, M., Crinelli, R., Carloni, E., Bianchi, M., Giacomini, E., Valbusa, U., Magnani, M., 2010. Biosensors and Bioelectronics 25, 2490–2496.
Pan, Q., Zhang, R., Bai, Y., He, N., Lu, Z., 2008. Analytical Biochemistry 375, 179–186.
Papavassiliou, A.G., 1995. New England Journal of Medicine 332, 45–47.
Perkins, N.D., 2007. Nature Reviews Molecular Cell Biology 8, 49–62.
Reymond, J.L., Koch, T., Schroder, J., Tierney, E., 1996. Proceedings of the National Academy of Sciences of the United States of America 93, 4521–4522.
Schmid, R.M., Liptay, S., Betts, J.C., Nabel, G.J., 1994. Journal of Biological Chemistry 269, 32162–32167.
Shao, F., Barton, J.K., 2007. Journal of the American Chemical Society 129, 14733–14738.
Sharp, M., Petersson, M., Edstrom, K., 1979. Journal of Electroanalytical Chemistry 95, 123–130.
Shen, M., Yang, M., Li, H., Liang, Z.Q., Li, G.X., 2012. Electrochimica Acta 60, 309–313.
Wang, J., Li, M.L., Hua, D., Chen, Q., 2006. Biotechniques 41, 79–88.
Wang, Z.H., Gidwani, V., Zhang, D.D., Wong, P.K., 2008. Analyst 133, 998–1000.
Zhou, H., Sun, Z.Y., Hoshi, T., Kashiwagi, Y., Anzai, J.I., Li, G., 2005. Biophysical Chemistry 114, 21–26.